

Cite this: *J. Mater. Chem. A*, 2021, 9, 7556

In situ construction of phenanthroline-based cationic radical porous hybrid polymers for metal-free heterogeneous catalysis†

Guojian Chen,[✉]* Yadong Zhang, Ke Liu, Xiaoqing Liu, Lei Wu, Hu Zhong, Xuejing Dang, Minman Tong[✉] and Zhouyang Long[✉]*

Rational design of multifunctional radical porous polymers with redox activity for targeted metal-free heterogeneous catalysis is an important research topic. In this work, we reported a new class of phenanthroline-based cationic radical porous hybrid polymers (Phen^{•+}-PHPs), which were constructed from the Heck reaction between a newly designed dibromo-substituted phenanthroline ionic monomer (iDBPhen) and a rigid building block, octavinylsilsesquioxane (VPOSS). For the first time, the stable phenanthroline-based radical cation was unexpectedly discovered in these polyhedral oligomeric silsesquioxane (POSS)-based porous hybrid polymers, probably undergoing *in situ* reduction of the dicationic monomer iDBPhen during the alkaline reagent K₂CO₃-involved Heck reaction. The radical characters of the typical porous polymers Phen^{•+}-PHP-2 and Phen^{•+}-PHP-2Br were confirmed from the electron paramagnetic resonance (EPR) spectra and X-ray photoelectron spectra (XPS). The chemical structures and porous geometry were fully characterized by a series of advanced technologies. Surprisingly, the metal-free cationic radical polymer Phen^{•+}-PHP-2 exhibited high heterogeneous catalytic efficiency in the H₂O₂-mediated selective oxidation of various sulfides to sulfoxides with high yields under mild conditions, owing to the electron-accepting and redox ability of Phen-based dications and radical cations. Moreover, the extended sample Phen^{•+}-PHP-2Br prepared by post-treatment of Phen^{•+}-PHP-2 with aqueous HBr was also employed as a metal-free efficient heterogeneous catalyst in the conversion of CO₂ with epoxides into cyclic carbonates under atmospheric pressure and low temperatures. The remarkable catalytic performance in CO₂ conversion should be assigned to the synergistic catalysis of POSS-derived Si–OH groups and nucleophilic Br[−] anions and N active atom-involved Phen cationic radical moieties within Phen^{•+}-PHP-2Br. These two catalysts can be facilely recovered and reused, also with stable recyclability in the above catalytic reaction systems, achieving the heterogeneous catalytic demands for multipurpose reactions.

Received 11th December 2020
Accepted 15th February 2021

DOI: 10.1039/d0ta12018a

rsc.li/materials-a

Introduction

Multivariate porous organic materials, in which diverse organic functional groups are incorporated into their skeletons, are capable of catalysis, adsorption, separation, energy storage and conversion.^{1,2} As kinds of attractive functional moieties, organic radicals are active species with unpaired electrons, which have drawn great interest in many fields due to their unique properties in optical, electrical, magnetic, redox and catalysis aspects.^{3–5} Recently, various organic radicals have been considered as building blocks for achieving functional purely organic porous materials including radical-type porous organic

polymers (POPs)^{6–9} and covalent organic frameworks (COFs).^{10–12} So far, most of the reported radical porous polymers mainly focused on applications in magnets and electric energy storage.^{8–11} However, few of such type porous polymers were applied to metal-free heterogeneous catalysis, which can afford much greener, economical and sustainable catalytic processes.

At present, most of the reported radical-type POPs were derived from neutral radicals such as triphenylmethyl (TPM) and 2,2,6,6-tetramethylpiperidine-*N*-oxyl (TEMPO) radicals or their derivatives.^{8,10,11} Among them, a great variety of TEMPO-based polymers have been used as effective catalysts for oxidation conversion of organic groups.¹³ In contrast with neutral radicals, cationic radicals are another example of radicals with diverse redox-driven changes for exploring more catalytic applications. Viologen radical cations are considered among the most stable organic radicals, which are obtained by means of chemical or electrical one-electron reductions of 4,4'-bipyridinium dications.¹⁴ Recently, viologen moieties have been

School of Chemistry and Materials Science, Jiangsu Key Laboratory of Green Synthetic Chemistry for Functional Materials, Jiangsu Normal University, Xuzhou, 21116, Jiangsu, China. E-mail: gjchen@jsnu.edu.cn; longzhouyangfat@163.com

† Electronic supplementary information (ESI) available. See DOI: 10.1039/d0ta12018a

incorporated into some POPs,^{15–24} only some of which exhibit stable cationic radical characters.^{18,21,23} These viologen-based ionic POPs were regarded as efficient heterogeneous catalysts in the conversion of CO₂ into cyclic carbonates,^{19,20,22,23} but rarely used in the liquid-phase catalytic oxidation reactions,²⁴ which are an important and valuable class of organic transformations. Therefore, it becomes an urgent need to develop new-type redox-oriented cationic radical porous polymers with versatile properties as metal-free catalysts for the targeted reactions.

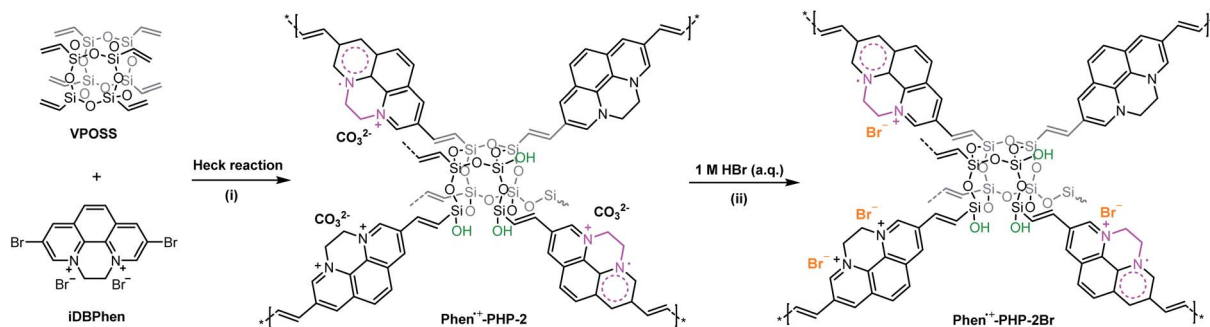
Herein, we reported *in situ* construction of multifunctional cationic radical porous polymers from ionic precursors *via* a one-pot and one-step process. As depicted in Scheme 1, a new class of phenanthroline-based cationic radical porous hybrid polymers (denoted as Phen^{•+}-PHPs) were synthesized from the Heck reaction between a newly-designed phenanthroline ionic monomer (iDBPhen) and a rigid unit octavinylsilsesquioxane (VPOSS). To our delight, for the first time, phenanthroline-based radical cations were discovered in the obtained Phen^{•+}-PHPs, which were formed by *in situ* reduction of iDBPhen during the K₂CO₃-involved one-pot process. The core building block VPOSS has an organic–inorganic hybrid structure with inorganic siloxane cages with reactive vinyl groups, which not only play an important part in fabricating robust porous organic–inorganic hybrid polymers with a hydrophobic reaction micro-environment but also afford POSS *in situ* derived Si–OH groups that can be beneficial for the catalytic reactions.^{22,23,25} Recently, some phenanthroline (Phen)-based neutral porous organic polymers have been reported as porous ligands for coordinating metal complexes for heterogeneous catalysis,^{26,27} but Phen-based ionic or radical polymers have not appeared as yet for metal-free catalysis. In this work, the typical porous polymer Phen^{•+}-PHP-2 possesses the remarkable radical and redox character, which was regarded as an efficient metal-free heterogeneous catalyst in H₂O₂-mediated selective oxidation of sulfides to sulfoxides at low temperatures. Towards metal-free catalytic CO₂ fixation, the extended catalyst Phen^{•+}-PHP-2Br prepared by acid post-treatment of Phen^{•+}-PHP-2 with the HBr aqueous solution afforded very high catalytic activities in the conversion of CO₂ with epoxides into various cyclic

carbonates under mild conditions. The good catalytic performance should be attributed to the synergistic catalytic effect of POSS-derived Si–OH groups and Br[–] anions and N active atoms involving Phen radical cations within the catalyst.

Results and discussion

Formation and characterization of Phen^{•+}-PHPs

Scheme 1 illustrates the synthetic process of Phen-based cationic radical porous hybrid polymers Phen^{•+}-PHPs. First, the typical Phen^{•+}-PHP-2 was fabricated from the one-pot Heck reaction between iDBPhen and rigid VPOSS units. This newly designed ionic precursor iDBPhen was prepared by the quaternization reaction of 3,8-dibromo-1,10-phenanthroline and 1,2-dibromoethane, which was found to be reduced into cationic radical Phen^{•+} moieties within polymers due to the use of the alkaline reagent K₂CO₃ as an HBr absorbent in the Heck reaction.²³ Meanwhile, bromide anions (Br[–]) within the ionic monomers can be also exchanged by the carbonate anions (CO₃^{2–}). Subsequently, Br[–] anion-paired Phen^{•+}-PHP-2Br can be obtained by acid post-treatment of the typical sample Phen^{•+}-PHP-2 in 1 M HBr aqueous solution. The experimental and characterization details for the synthesis of iDBPhen (Fig. S1†), two control phenanthroline-based ionic monomers (iPhen-1 and iPhen-2, Scheme S1, Fig. S2 and S3†) and Phen^{•+}-PHPs (Scheme S2†) can be found in the ESI.† X-ray diffraction (XRD) patterns reveal that both iDBPhen and VPOSS are crystalline monomers (Fig. S4†), but the obtained polymers Phen^{•+}-PHPs are amorphous forms (Fig. S5†), indicating the formation of disordered three-dimensional network polymers by highly crosslinking VPOSS with iDBPhen.^{23,25} As a result, the above Phen^{•+}-PHPs are insoluble in common organic solvents such as tetrahydrofuran (THF), *N,N*-dimethylformamide (DMF) and dimethyl sulfoxide (DMSO), indicating their robust and highly cross-linked structures. As shown in the thermogravimetric analysis (TGA) curves (Fig. S6†), the typical samples Phen^{•+}-PHP-2 and Phen^{•+}-PHP-2Br exhibit good thermal stability up to 300 °C under an air atmosphere, even better than that of VPOSS. Besides, Phen^{•+}-PHP-2 and Phen^{•+}-PHP-2Br show improved hydrophilic properties compared with the hydrophobic VPOSS by the introduced hydrophilic Phen ionic moieties, which can



Scheme 1 Synthetic routes to typical phenanthroline-based cationic radical porous hybrid polymers Phen^{•+}-PHP-2 and Phen^{•+}-PHP-2Br. (i) Heck reaction conditions: VPOSS/iDBPhen = 1/2, the catalyst Pd(PPh₃)₄, K₂CO₃, DMF/H₂O, 120 °C, 72 h; (ii) post-treatment by aqueous HBr at room temperature for 12 h.

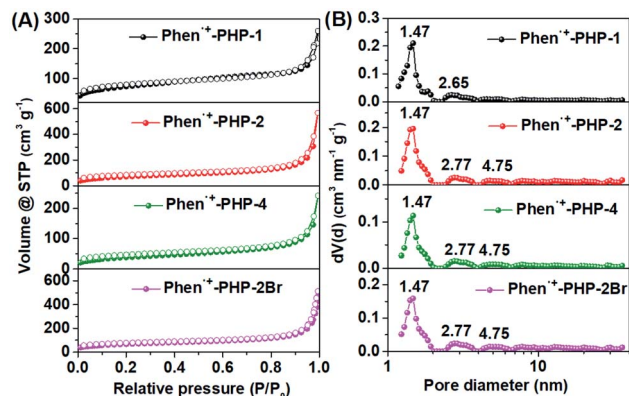


Fig. 1 (A) N_2 adsorption–desorption isotherms and (B) NLDFT pore size distributions of Phen⁺-PHP- x ($x = 1, 2, 4$) and Phen⁺-PHP-2Br.

stably absorb a small amount of water nearby ionic sites, which is reflected by the initial losses of weight (*ca.* 5–7 wt%) up to 200 °C in the TGA curves (Fig. S6†).^{28–30}

Porous textural properties and contents of Phen moieties for Phen⁺-PHP- x can be tailored by varying molar ratios of iDBPhen to VPOSS ($x = 1, 2$ and 4). The porous structures of Phen⁺-PHPs were analyzed by the N_2 adsorption–desorption measurement (Fig. 1A), and the textural properties, N contents (wt%) and Phen content (mmol g^{-1}) of Phen⁺-PHPs series are summarized in Table 1. As depicted in Fig. 1A, all the Phen⁺-PHP- x exhibit type II and IV isotherms with certain uptakes (22–45 $\text{m}^3 \text{g}^{-1}$) at low relative pressures ($P/P_0 < 0.01$) and obviously increasing ones at higher relative pressures ($0.80 < P/P_0 < 0.99$), indicating the coexistence of micropores and mesopores. The nonlocalized density functional theory (NLDFT) pore size distributions (Fig. 1B) of Phen⁺-PHP- x further demonstrate their hierarchical porous structures with micropores narrowly centered at 1.47 nm and mesopores randomly appearing at 2.65–4.75 nm. With the increase of $x = 1$ to 4 in the synthesis menus, the BET surface areas (S_{BET}) and total pore volume (V_{total}) gradually decrease, while the N and Phen contents in Phen⁺-PHP- x remarkably increase from 3.84 to 9.95 wt% and 1.37 to 3.55 mmol g^{-1} , respectively. Besides, the micropore surface areas (S_{micro}) and micropore volumes (V_{micro}) are

obviously decreasing with the increasing of x values, contributing to about 42–51% of S_{BET} values and only 6–16% of V_{total} values. These results imply that Phen⁺-PHP- x series have enriched mesoporosities, which are beneficial to the mass transfer of reactants to come into contact with the catalysts in the reactions. Obviously, the sample Phen⁺-PHP-2 has a higher S_{BET} value of 266 $\text{m}^2 \text{g}^{-1}$, the highest V_{total} of 0.881 $\text{cm}^3 \text{g}^{-1}$ with abundant large-size mesopores, and moderate N content (6.38 wt%) and Phen content (2.28 mmol g^{-1}), which would be used as the desired heterogeneous catalyst. After the post-treatment with aqueous HBr, the corresponding Br[−] anion-paired Phen⁺-PHP-2Br exhibits a slightly decreased S_{BET} value of 245 $\text{m}^2 \text{g}^{-1}$, a V_{total} value of 0.796 $\text{cm}^3 \text{g}^{-1}$ and a Phen content of 1.88 mmol g^{-1} , due to the introduction of bulky Br[−] anions. In addition, a control neutral porous hybrid polymer Phen-PHP-2 (seen the porous structure in Fig. S7†) has a rather high S_{BET} value of 491 $\text{m}^2 \text{g}^{-1}$ and an ultrahigh V_{total} value of 1.570 $\text{cm}^3 \text{g}^{-1}$. In addition, the porous morphology of Phen⁺-PHP-2 and Phen⁺-PHP-2Br was observed by scanning electron microscopy (SEM) and transmission electron microscopy (TEM). As shown in Fig. S8,† both of them have the fluffy cotton-like morphology and abundant mesoporosity, which originated from the interconnected nanoparticles.

The chemical structures and radical characters of Phen⁺-PHPs were confirmed by a series of characterization studies including solid-state ^{13}C cross-polarization magic-angle spinning (CP-MAS) and ^{29}Si MAS NMR spectra, UV-Vis spectra, electron paramagnetic resonance (EPR) spectra, Fourier transform infrared (FTIR) spectra and X-ray photoelectron spectroscopy (XPS). In the ^{13}C CP-MAS NMR spectra (Fig. 2A) of Phen⁺-PHP-2 and Phen⁺-PHP-2Br, the multiple resonance peaks centered at 128.3 and 129.2 ppm correspond to the aromatic carbons from Phen moieties and silicon-based ethylene carbons (Si-CH=CH-) from VPOSS units.^{23,25–27,31} The small peaks appearing at around 159 ppm are assigned to N-bonded carbon atoms in Phen units.^{26,27} The peaks with low chemical shifts at around 51.0 ppm and 41.2–42.6 ppm correspond to the ethylene carbons that can bridge the two N atoms in a Phen unit, which can be found at similar positions in the liquid-state ^{13}C NMR spectra of iDBPhen and iPhen-1 (Fig. S1B and S2B†). These results demonstrate the successful formation of POSS-based

Table 1 Textural properties of Phen⁺-PHP- x series, Phen⁺-PHP-2Br and the control neutral polymer Phen-PHP-2

Samples ^a	$n(\text{VPOSS}) : n(\text{iDBphen})$	S_{BET}^b ($\text{m}^2 \text{g}^{-1}$)	S_{micro}^c ($\text{m}^2 \text{g}^{-1}$)	V_{micro}^c ($\text{cm}^3 \text{g}^{-1}$)	V_{total}^d ($\text{cm}^3 \text{g}^{-1}$)	D_p^e (nm)	N content ^f (wt%)	Phen content ^g (mmol g^{-1})
Phen ⁺ -PHP-1	1 : 1	267	135	0.064	0.401	1.47, 2.65	3.84	1.37
Phen ⁺ -PHP-2	1 : 2	266	119	0.054	0.881	1.47, 2.77	6.38	2.28
Phen ⁺ -PHP-4	1 : 4	142	60	0.027	0.375	1.47, 2.77	9.95	3.55
Phen ⁺ -PHP-2Br	1 : 2	245	121	0.056	0.796	1.47, 2.77	5.27	1.88
Phen-PHP-2 ^h	1 : 2	491	285	0.130	1.570	1.23, 2.77	4.29	1.53

^a Phen⁺-PHP- x was obtained from the Heck reaction of VPOSS with iDBPhen using different molar ratios ($x = 1, 2$ and 4). ^b BET surface area calculated over the range $P/P_0 = 0.05–0.20$. ^c Micropore surface area and pore volume calculated by the t -plot method. ^d Total pore volume calculated at $P/P_0 = 0.99$. ^e The main pore diameters calculated using NLDFT theory. ^f The N content (wt%) obtained by the CHN elemental analysis. ^g Phen content (mmol g^{-1}) = $0.5 \times 1000 \times \text{N content (wt\%)/14}$. ^h For synthesis of Phen-PHP-2 (see the detailed process in Scheme S2), the molar ratio of $n(\text{VPOSS})$ to $n(\text{DBPhen})$ is 1 : 2.

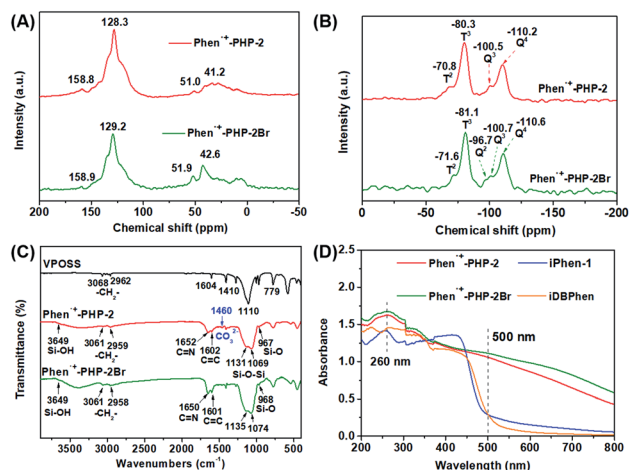


Fig. 2 The solid-state (A) ^{13}C CP-MAS NMR spectra and (B) ^{29}Si MAS spectra of Phen $^{+}$ -PHP-2 and Phen $^{+}$ -PHP-2Br, (C) FTIR spectra of VPOSS, Phen $^{+}$ -PHP-2, Phen $^{+}$ -PHP-2Br, and (D) UV-Vis spectra of Phen $^{+}$ -PHP-2, Phen $^{+}$ -PHP-2Br, iDBPhen and iPhen-1.

Phen-linked porous polymers. The ^{29}Si MAS NMR spectra (Fig. 2B) indicate that T^n [$\text{CSi}(\text{OSi})_n(\text{OH})_{3-n}$] and Q^m [$\text{Si}(\text{OSi})_m(\text{OH})_{4-m}$] silicon units co-existed in the samples of Phen $^{+}$ -PHP-2 and Phen $^{+}$ -PHP-2Br. The main signals at -80.3 and -81.1 ppm are assigned to silicon atoms of the retained cubic T^3 units; 23,25,31 the affiliated peaks at -70.8 and -71.6 ppm are attributed to the newly-formed T^2 units that arise from the partial collapse of T^3 units by the cleavage of Si–O–Si bonds. 15,23,32 For Phen $^{+}$ -PHP-2, obvious signals appearing at -100.5 and 110.2 ppm suggest the formation of Q^3 and Q^4 silicon units, 31,32 which are caused by the cleavage of Si–C bonds of T^3 units and further self-condensation of Si–OH contained Q^3 units. 15,22,33 Besides, there are only slight differences of Q^n units for Phen $^{+}$ -PHP-2Br, *i.e.*, a small peak at -96.7 ppm is assigned to the Q^2 unit, 22,23 due to further decomposition of Q^3 silicon units by post-treatment in HBr aqueous solution. According to the FTIR spectra in Fig. 2C, compared with one sharp peak for the typical Si–O–Si asymmetric stretching vibration at 1110 cm^{-1} for cubic VPOSS, 33,34 such peaks along with some splits and broad shifts for Phen $^{+}$ -PHP-2 and Phen $^{+}$ -PHP-2Br appear at 1131 , 1069 cm^{-1} and 1135 , 1074 cm^{-1} , suggesting the coexistence of T^n and Q^n silicon units. 22,23,25 The existence of Si–OH groups in Phen $^{+}$ -PHPs was indicated from the Si–OH and Si–O stretching vibrations that appeared at 3649 cm^{-1} and 967 cm^{-1} . 22 In addition, the successful introduction of Phen parts was confirmed by the new bands located at around 1652 and 1602 cm^{-1} assigned to C=N and C=C stretching vibrations. 27,35 As a result, the above formed T^2 , Q^2 and Q^3 units should be attributed to the destruction and distortion of cubic POSS cages by the cleavage of Si–C and Si–O bonds during the highly cross-linked process, just affording enriched Si–OH groups for the subsequent catalytic reactions.

Furthermore, the solid-state UV-Vis and EPR spectroscopies confirm the formation of Phen radical cations within Phen $^{+}$ -PHP-2 and Phen $^{+}$ -PHP-2Br. In detail, UV-Vis spectra (Fig. 2D) recorded for Phen $^{+}$ -PHP-2 and Phen $^{+}$ -PHP-2Br show obvious

broad absorbing bands in the range of $500\text{--}800\text{ nm}$ compared with iDBPhen and iPhen-1 monomers, which are characteristic of Phen radical cations. EPR spectra (Fig. 3A) provide direct evidence for proving the existence of Phen radicals. The samples Phen $^{+}$ -PHP-2 and Phen $^{+}$ -PHP-2Br both exhibit sharp peaks with similar g factors (2.0026 and 2.0023), indicative of the newfound Phen organic radicals with unpaired electrons, which are similar to the common viologen radicals. 12,18,21,23 As expected, the EPR signals for two control dicationic monomers iDBPhen and iPhen-1 are silent, indicating the absence of radicals in the dicationic precursors. These compared results reveal that cationic radical Phen $^{+}$ -PHPs are formed by *in situ* reduction of the dicationic iBPhen during the alkaline reagent K_2CO_3 -involved Heck reaction without using additional reducing agents (*e.g.*, $\text{Na}_2\text{S}_2\text{O}_4$). 12,36 Indeed, some recent reports have given some clues to form viologen cationic radicals under alkaline conditions, which are demonstrated again in the present Phen-based cationic radical polymers. 21,23

The chemical states and compositions of Phen $^{+}$ -PHPs were further confirmed using the XPS technique. The full survey XPS spectra (Fig. 3B) show the elemental compositions of C, N, O and Si for Phen $^{+}$ -PHP-2, and C, N, O, Si and Br for Phen $^{+}$ -PHP-2Br. To our surprise, the residual Br element in Phen $^{+}$ -PHP-2 was negligible, demonstrating that bromo-substituted iDBPhen monomers were fully consumed in the Heck reaction, and Br^- anions within iDBPhen ionic monomers were also exchanged by CO_3^{2-} anions from K_2CO_3 . The presence of CO_3^{2-} anions was also reflected by a small FTIR adsorbed peak (O–C–O) at 1460 cm^{-1} (Fig. 2C) and a divided O–C–O peak at 286.9 eV in the high-resolution C 1s XPS spectrum of Phen $^{+}$ -PHP-2 (Fig. 3E). 37,38 Besides, very small amounts of residual metal Pd (*ca.* $0.1\text{ wt}\%$) within Phen $^{+}$ -PHP-2 and Phen $^{+}$ -PHP-2Br were detected by both XPS and inductively coupled plasma mass spectrometry (ICP-MS), due to the lack of free N atom containing Phen ligands. The subsequent control experiments would further indicate that the residual Pd has negligible influence on the targeted catalytic reactions, which are different from other trapped trace metal Pd-catalyzed organic transformations. 39,40 Based on the aforementioned cationic radical characters for the Phen $^{+}$ -PHPs, three electronic states for N atoms were recognized from the divided peaks from the N 1s spectra (Fig. 3D). For Phen $^{+}$ -PHP-2, the small peak located at 401.3 eV originated from the N atoms of dicationic Phen moieties (Phen N^{++}) and the two relatively higher peaks at 399.9 and 398.8 eV can be attributed to the N atoms in the cationic radical Phen species (Phen $\text{N}^{\cdot+}$) and further reduced neutral Phen N^0 , respectively. 6,23 For the Phen $^{+}$ -PHP-2, the fitting area ratios of Phen N^{++} , Phen $\text{N}^{\cdot+}$ and Phen N^0 are 0.253 , 0.378 and 0.369 , implying that most of the dicationic iDBPhen was *in situ* reduced to cationic radical and neutral forms during the K_2CO_3 -involved Heck reaction. These two plausible reversible redox states related to Phen $^{+}$ and Phen 0 *via* one- and two-electron reductions of the model ionic precursor iPhen-1 are described in Scheme S3, † similar to the reversible redox processes of viologens and derivatives. 12,14,24 By acid post-treatment of Phen $^{+}$ -PHP-2 with 1 M HBr aqueous solution, as is well known, CO_3^{2-} anions were easily removed by reacting with excess acidic H^+ and subsequently replaced by Br^-

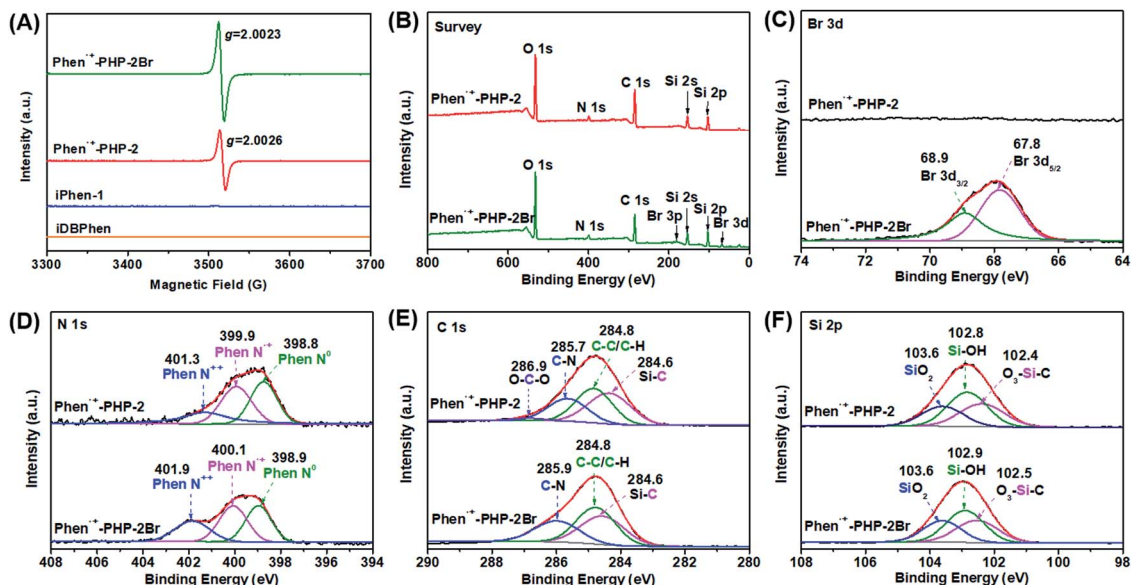


Fig. 3 (A) EPR spectroscopy of Phen⁺-PHP-2 and Phen⁺-PHP-2Br and their XPS spectra: (B) survey, (C) Br 3d, (D) N 1s, (E) C 1s, and (F) Si 2p.

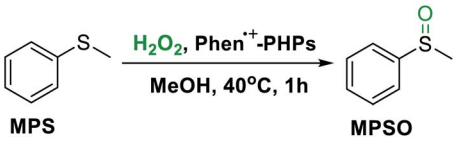
anions *via* anion-exchange, and the obtained Phen⁺-PHP-2Br has obviously increased Br⁻ anions, which was displayed by Br 3d_{3/2} and Br 3d_{5/2} at 68.9 and 67.8 eV in the Br 3d spectrum (Fig. 3C).^{23,25} Phen⁺-PHP-2Br still exhibits the radical character with multiple Phen N forms, similar to its precursor Phen⁺-PHP-2. The fitting ratios of these three Phen N forms change slightly, that is, some Phen N⁺ and Phen N⁰ return to Phen N⁺⁺ after HBr acid treatment.²¹ The molar ratio of dicationic Phen N⁺⁺ paired with Br⁻ anions is about 0.269, while the value for Phen N⁺ is 0.376. Besides, the C 1s spectra (Fig. 3E) can be mainly fitted to three peaks at 285.9 (C-N), 284.8 (C-C/C-H) and 284.6 eV (Si-C), which are assigned to the carbon atoms in Phen moieties, methylene groups and POSS units.^{23,25} Three types of electronic states of silicon atoms were confirmed from the high-resolution Si 2p spectra (Fig. 3F). Taking Phen⁺-PHP-2Br as the example, the Si 2p peak at 102.5 eV can be assigned to the Si atoms within T³ units (*i.e.*, O₃-Si-C);^{23,25,41} the main peak located at 102.9 eV should be attributed to Si-OH groups derived from T³, Q², and Q³ silicon units; the Si 2p peaks at the higher value of 103.6 eV are assigned to Q⁴ silicon atoms (SiO₂).^{23,25,31} These multiple electron states of Si atoms again demonstrate the co-existence of Tⁿ and Qⁿ units with Si-OH groups in Phen⁺-PHPs, which can be regarded as hydrogen bond donors (HBDs) for enhancing catalytic efficiency in CO₂ conversion.^{23,25}

Metal-free oxidation of sulfides catalyzed by Phen⁺-PHPs

Owing to the radical and redox characters of Phen⁺-PHPs, they were applied as metal-free heterogeneous catalysts in the oxidation of sulfides using hydrogen peroxide (H₂O₂) as a green oxidant, which can produce many important fine chemicals.⁴² Most of the effective catalysts for these oxidation reactions mainly depend on metal active species such as polyoxometalates.^{43,44} Although several electron-deficient

heterocyclic organic salts have been reported as homogeneous organocatalysts for the oxidation of sulfides,⁴⁵⁻⁴⁷ there are few examples of metal-free heterogeneous catalysts for achieving such oxidations,^{24,48,49} making this work challenging. First, the typical sample Phen⁺-PHP-2 was used as a metal-free heterogeneous catalyst in selective oxidation of the model substrate methyl phenyl sulfide (MPS) with 30 wt% H₂O₂. Very surprisingly, the product methyl phenyl sulfoxide (MPSO) was smoothly obtained with both a high yield and selectivity of 99% (Table 2, entry 1) under mild conditions (*i.e.*, near room temperature 40 °C for only 1 h) along with a high turnover frequency (TOF) value of 21.7 h⁻¹. Besides, the catalyst Phen⁺-PHP-2 can be used at least three times without obvious loss of catalytic activities, indicating its heterogeneous nature and good stability. It was found that Br⁻ anion-paired Phen⁺-PHP-2Br also achieved good conversion of MPS to MPSO with a high yield of 99% and a high TOF value of 26.3 h⁻¹ as well as Phen⁺-PHP-2. This result suggests that the type of counter anions has no obvious influence on catalytic oxidation activities. In order to determine the exact catalytically active site responsible for the oxidation activity, several control catalysts were prepared. When the neutral polymer Phen-PHP-2 and Phen monomer were used as catalysts in the reaction (Table 2, entries 3 and 4), MPSO yields of 56% and 58% were obtained, but these values were very close to the yield of 54% in a blank run without using catalysts and only adding the oxidant H₂O₂ (Table 2, entry 10). These equal results indicate that neutral Phen moieties have negligible contributions to accelerate the catalytic oxidation activity. In contrast, dicationic monomers iDBPhen and iPhen-1 (see in Scheme S1†) with ethylene bridges can efficiently catalyze this oxidation, affording high yields of 98% and 87% and desired TOF values (Table 2, entries 5 and 6). However, the monocationic monomer iPhen-2 tethered with an ethane group only gave a low yield of 56%, close to the value in

Table 2 Selective oxidation of methyl phenyl sulfide (MPS) to methyl phenyl sulfoxide (MPSO) catalyzed by Phen⁺⁺-PHPs and control catalysts^a



Entry	Catalyst	Yield ^b (%)	Selectivity ^b (%)	TOF value ^c (h ⁻¹)
1	Phen ⁺⁺ -PHP-2	99/98/95 ^d	99	21.7
2	Phen ⁺⁺ -PHP-2Br	99	99	26.3
3	Phen-PHP-2	56	99	—
4	Phen ^e	58	99	—
5	iDBPhen ^e	98	99	21.6
6	iPhen-1 ^e	87	99	19.1
7	iPhen-2 ^e	56	99	—
8	K ₂ CO ₃ ^f	52	99	—
9	Pd(PPh ₃) ₄ ^g	58	99	—
10	Blank ^h	54	99	—

^a Reaction conditions: MPS (1 mmol), 30 wt% H₂O₂ (2 mmol), the catalyst (20 mg), the solvent MeOH (4 mL), temperature (40 °C), time (1 h). ^b Yield and selectivity of MPSO were determined by ¹H NMR analyses (see the spectrum in Fig. S9). ^c Turnover frequency (TOF) = [mmol (product)]/[mmol (Phen content in the catalyst) × reaction time (h)]. ^d The yields were obtained by the recovery of the catalyst for three runs. ^e The dosages of ionic Phen (iPhen-1 and iPhen-2) and 1,10-phenanthroline (Phen) monomers were calculated based on Phen contents of Phen⁺⁺-PHP-2 and Phen-PHP-2. ^f The dosage of K₂CO₃ was 10 mg. ^g The dosage of Pd(PPh₃)₄ was 0.02 mg based on the Pd content in Phen⁺⁺-PHP-2. ^h The blank experiment was conducted without using catalysts only using 30 wt% H₂O₂.

the blank reaction. These interesting compared results reveal that the ethylene bridges within dicationic Phen organic salts are vital for electron transfer in reversible redox states between Phen⁺⁺ and Phen N⁺ species (Scheme S3†), but the ethane group cannot play such a role of electronic bridges for the redox reactions. Besides, the control reagent K₂CO₃ and Pd(PPh₃)₄ have not obviously improved catalytic activities (Table 2, entries 8 and 9) compared with the blank experiment, revealing the absence of catalytic roles of CO₃²⁻ anions and residual trace Pd within Phen⁺⁺-PHP-2. As a result, these above comparisons definitely confirm that the true active sites for catalyzing such an oxidation reaction are dicationic or cationic radical Phen moieties. To the best of our knowledge, it was the first time to discover that dicationic and cationic radical Phen salts can be regarded as metal-free catalysts for the oxidation reactions. In a word, the catalyst Phen⁺⁺-PHP-2 exhibited the optimal catalytic activity in H₂O₂-mediated oxidation of MPS under mild conditions, which was much better than that of a recently reported viologen-based heterogeneous catalyst PIN-1,²⁴ and was even comparable to many reported metal-based heterogeneous catalysts (see Table S1† for details).^{43,44}

From the view of green chemistry, the metal-/halogen-free catalyst Phen⁺⁺-PHP-2 was more suitable for the selective oxidation of sulfides with H₂O₂. To evaluate the substrate scope of Phen⁺⁺-PHP-2, catalytic oxidation of various sulfides was carried out under mild conditions (Table 3). The catalyst

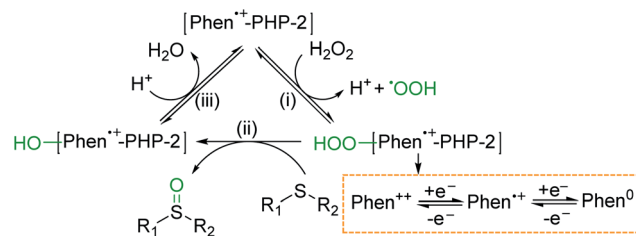
Table 3 Substrate scope for selective oxidation of sulfides with H₂O₂ over the catalyst Phen⁺⁺-PHP-2^a

Entry	Substrate	Product	T (°C)	t (h)	Yield ^b (%)
1			40	2	99
2			40	1	99
3			40	2	99
4			60	6	93
5			60	6	96
6			60	6	90

^a Reaction conditions: sulfide (1 mmol), 30 wt% H₂O₂ (2 mmol), the catalyst Phen⁺⁺-PHP-2 (20 mg), the solvent MeOH (4 mL), temperature (T = 40–60 °C), time (t = 1–6 h). ^b Yields were determined from ¹H NMR spectra (Fig. S10–S15) of the crude sulfoxides. The selectivities of the sulfoxides are over 99%.

Phen⁺⁺-PHP-2 showed good catalytic activities in the oxidation of MPS analogues with electron-donating groups (–CH₃, –OCH₃ and –OH) located in *para*-positions, giving the corresponding sulfoxides with high yields of 99% (Table 3, entries 1–3) under very mild conditions at 40 °C for 1–2 h. Especially, the relatively inert sulfides with electron-withdrawing groups (–F, –Cl and –Br) could be also transformed into the corresponding sulfoxides with desired yields of 90–96% (Table 3, entries 4–6) at a higher temperature of 60 °C for 6 h. As a result, Phen⁺⁺-PHP-2 has been proved as an efficient metal-free heterogeneous catalyst for achieving the oxidation conversion of various sulfides to sulfoxides under mild conditions.

Based on previous findings in H₂O₂-mediated oxidations of sulfides over metal-free organocatalysts such as pyrazinium or heteroarenium salts,^{45–47} a possible reaction mechanism for the catalyst Phen⁺⁺-PHP-2 is proposed in Scheme 2. First, when the catalyst Phen⁺⁺-PHP-2 reacted with the oxidant H₂O₂, the activated H₂O₂ transforms into active species [•]OOH by an electron transfer process of Phen⁺⁺ or Phen^{•+} with the formation of Phen radical cations or neutral forms, thus leading to the formation of a Phen-hydroperoxide adduct.^{24,45–47} Then, the oxidation of sulfide to sulfoxide was achieved by oxygen transfer from the Phen-hydroperoxide active species to the substrates.^{45–47} Finally, the catalyst Phen⁺⁺-PHP-2 was regenerated by the elimination of



Scheme 2 Proposed reaction mechanism for oxidation of sulfides with H_2O_2 catalyzed by $\text{Phen}^{++}\text{-PHP-2}$.

a hydroxyl group from a pseudobase and also release of the by-product water.^{45,47}

Metal-free catalytic CO_2 fixation over $\text{Phen}^{++}\text{-PHP-2Br}$

The chemical fixation of CO_2 with epoxides into value-added cyclic carbonates is a promising, atom economic and energy-saved non-redox route to achieve the utilization of such C1 resources.^{50–52} Owing to the multiple active sites including Phen cationic radical sites paired with Br^- anions and POSS-derived Si-OH groups, $\text{Phen}^{++}\text{-PHP-2Br}$ was further investigated as a metal-free heterogeneous catalyst in CO_2 conversion. First, the catalytic performances of both $\text{Phen}^{++}\text{-PHP-2}$ and $\text{Phen}^{++}\text{-PHP-2Br}$ were assessed in the cycloaddition of CO_2 with a model substrate epichlorohydrin (ECH) without using any solvents and co-catalysts under atmospheric pressure (0.1 MPa) using a CO_2 balloon (Table 4). At a low temperature of 60 °C for 48 h, the metal-/halogen-free catalyst $\text{Phen}^{++}\text{-PHP-2}$ only gave a low

Table 4 The CO_2 cycloaddition with ECH catalyzed by $\text{Phen}^{++}\text{-PHPs}$ under different conditions^a

Entry	Catalyst	T (°C)	t (h)	Yield ^b (%)	Selectivity ^b (%)
1	$\text{Phen}^{++}\text{-PHP-2}$	60	48	37	99
2	$\text{Phen}^{++}\text{-PHP-2}$	60	72	83	99
3	$\text{Phen}^{++}\text{-PHP-2Br}$	60	48	99	99
4	$\text{Phen}^{++}\text{-PHP-2Br}$	40	96	93	99
5	Phen-PHP-2	60	48	28	99
6	Phen-PHP-2	60	72	78	99
7	Phen^c	60	48	13	99
8	Phen^c	60	72	60	99
9	$\text{Phen}\cdot(\text{H}_2\text{O})^c$	60	72	82	97
10	iPhen-1 ^c	60	48	91	99
11	$\text{Pd}(\text{PPh}_3)_4^d$	60	48	Trace	—

^a Reaction conditions: ECH (2 mmol), CO_2 pressure (0.1 MPa), the catalyst (40 mg), temperature ($T = 40\text{--}60$ °C), time ($t = 48\text{--}96$ h).

^b Yield and selectivity of the cyclic carbonate determined by both GC and ^1H NMR (see the typical spectrum in Fig. S16); a small amount of by-product is 3-chloro-1,2-propanediol. ^c The dosages of iPhen-1, Phen and $\text{Phen}\cdot(\text{H}_2\text{O})$ are calculated based on the Phen content of $\text{Phen}^{++}\text{-PHP-2Br}$ and Phen-PHP-2 , respectively. ^d The dosage of $\text{Pd}(\text{PPh}_3)_4$ was 0.04 mg based on the trace Pd content in $\text{Phen}^{++}\text{-PHP-2Br}$.

yield of 37% for the product 4-(chloromethyl)-1,3-dioxolan-2-one, but could afford a moderate yield of 83% using a longer reaction time of 72 h (Table 4, entries 1 and 2). For comparison, the Br^- anion-paired catalyst $\text{Phen}^{++}\text{-PHP-2Br}$ provided an excellent yield of 99% and a perfect selectivity of 99% at 60 °C for 48 h (Table 4, entry 3) and still gave a desired yield of 93% at a lower temperature of 40 °C for 96 h (Table 4, entry 4). The above results suggest that nucleophilic Br^- anions are very important to remarkably enhance the catalytic activity in CO_2 conversion. In order to understand the true catalytic active sites within these two different catalysts $\text{Phen}^{++}\text{-PHP-2}$ and $\text{Phen}^{++}\text{-PHP-2Br}$, another control metal-/halogen-free catalyst neutral Phen-PHP-2 was carried out under similar conditions. At 60 °C for 48 h and 72 h, the catalyst Phen-PHP-2 also gave moderate yields of 28% and 78% (Table 4, entries 5 and 6) that were slightly lower than those of $\text{Phen}^{++}\text{-PHP-2}$. In order to assess the possible catalytic roles of POSS-derived Si-OH groups and N active sites, some well-designed control experiments were carried out as follows. Compared with the catalytic behaviors of $\text{Phen}^{++}\text{-PHP-2}$ and Phen-PHP-2 , the control anhydrous 1,10-phenanthroline (Phen) gave relatively lower yields of 13% and 60% at 60 °C for 48 h and 72 h (Table 4, entries 7 and 8), while an interesting catalyst 1,10-phenanthroline monohydrate $\text{Phen}\cdot(\text{H}_2\text{O})$ afforded an equal yield of 82% and a slightly decreased selectivity of 97% (Table 4, entry 9). As a result, one water molecule in $\text{Phen}\cdot(\text{H}_2\text{O})$ has a positive effect in enhancing the catalytic activity and only has a slight influence on the selectivity. These valuable comparisons indicate that N active atoms in Phen or Phen^{++} moieties in the catalysts have certain catalytic activities in such reactions. Moreover, the abundant OH groups from both Si-OH groups and a small amount of absorbed water molecules play a vital hydrogen bond donor (HBD) role in enhancing the catalytic activity; meanwhile, they do not obviously affect the product selectivity *via* a possible hydrolysis process, which has been reflected in the result using the control catalyst $\text{Phen}\cdot(\text{H}_2\text{O})$ and also revealed by some recent reports related to Si-OH or water-promoted HBD catalysis.^{23,25,53–56} Besides, no product was found over the control catalyst $\text{Pd}(\text{PPh}_3)_4$ (entry 11), which could exclude the possible influence on this catalytic reaction. Therefore, moderate catalytic activities over metal-/halogen-free heterogeneous catalysts $\text{Phen}^{++}\text{-PHP-2}$ and Phen-PHP-2 should be attributed to the synergistic combination of Phen-based free N or N^{++} active sites, POSS-derived Si-OH groups and a small amount of absorbed water within the catalysts.^{23,56–58}

In fact, the present metal-/halogen-free heterogeneous catalysts $\text{Phen}^{++}\text{-PHP-2}$ and Phen-PHP-2 still gave considerable catalytic activities in the conversion of CO_2 under ambient conditions, which could be comparable to those of recently reported metal-/halogen-free catalysts.^{59–62} To attain much better catalytic efficiency under milder conditions, the improved $\text{Phen}^{++}\text{-PHP-2Br}$ was the more suitable heterogeneous catalyst, even superior to the catalytic behavior over a homogeneous ionic monomer iPhen-1 (Table 4, entry 10). These results also confirm that Si-OH groups and inherent absorbed H_2O within $\text{Phen}^{++}\text{-PHP-2Br}$ work together with Br^- anions to achieve the good catalytic performance in CO_2 conversion with ECH, which

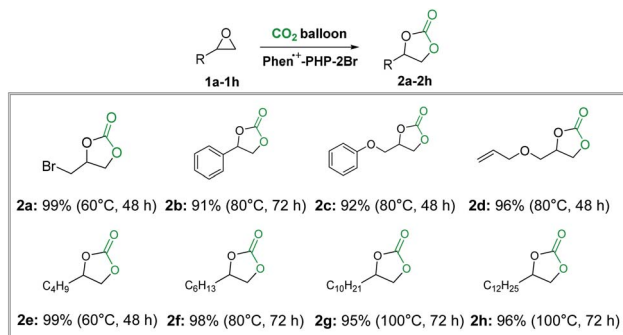
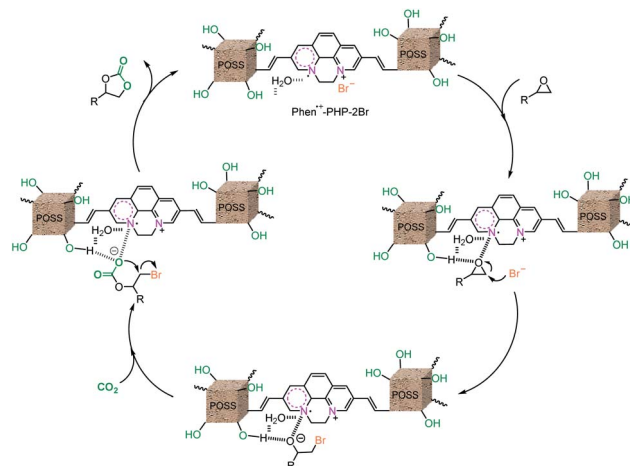


Fig. 4 Substrate scope for the cycloaddition of CO₂ with various epoxides catalyzed by Phen⁺-PHP-2Br. Reaction conditions: substrate (2.0 mmol), catalyst (40 mg), CO₂ (0.1 MPa), 60–100 °C, 48–72 h. The yields of cyclic carbonates were determined from the ¹H NMR spectra of crude products (Fig. S17–S24†).

was superior to those of many reported porous ionic polymers (PIPs)^{19,20,63–66} and was also comparable to those of metal-free PIPs with HBD groups (see Table S2† for details).^{22,23,25,56,67–70}

The optimal catalyst Phen⁺-PHP-2Br was further explored in the cycloaddition of CO₂ with various epoxides under atmospheric pressure. As shown in Fig. 4, the ECH analogue epibromohydrin **1a** could be smoothly converted to its cyclic carbonate **2a** with a high yield of 99% at 60 °C for 48 h. The commonly used substrates **1b–1d** (styrene oxide, glycidyl phenyl ether and allyl glycidyl ether) were also efficiently converted into the corresponding cyclic carbonates (**2b–2d**) with desired yields of 91–96% at a higher temperature of 80 °C. Notably, efficient transformation of long carbon chains with inert epoxides (**1e–1h**) could be well achieved in high yields (95–99%) of products (**2e–2h**) under different reaction conditions. The longer the carbon chains of substrates, the higher the temperatures or longer the reaction times needed in the reactions. In a word, Phen⁺-PHP-2Br has good substrate scope in the conversion of CO₂ with various epoxides. Besides, the robust recyclability and heterogeneous nature of the catalyst Phen⁺-PHP-2Br were investigated by a five-cycle assessment in CO₂ conversion with ECH that exhibited no obvious loss of catalytic activity (Fig. S25†). The chemical composition and structural morphology of the reused catalyst were assessed by characterization studies such as FTIR, XPS, N₂ sorption and SEM (Fig. S26–S28†), confirming its good structural stability.

Previous reports have revealed that nucleophiles (halogen anions) and electrophiles (*e.g.*, HBD groups) are beneficial for the activation and conversion of epoxides with CO₂.^{50,51,58} In this work, the designed “all-in-one” catalyst Phen⁺-PHP-2Br possesses multiple catalytically active sites including Phen-based cationic radical sites with Br[−] anions and N active atoms, POSS-derived Si–OH groups and H-bonded water molecules, which together account for the high catalytic activity by synergistic catalytic effect. Besides, the catalyst also has a moderate surface area, abundant mesoporosity and a suitable POSS-constructed hydrophobic reaction micro-environment, which can improve the mass transfer of large-sized long-chain hydrophobic epoxides to smoothly contact catalytic active



Scheme 3 A plausible synergistic catalytic mechanism for the conversion of CO₂ with epoxides over the “all-in-one” catalyst Phen⁺-PHP-2Br.

sites.^{23,25} Furthermore, the moderate CO₂ adsorption capacities of Phen⁺-PHPs (*i.e.*, 1.28 mmol g^{−1} for Phen⁺-PHP-2 and 0.89 mmol g^{−1} for Phen⁺-PHP-2Br at 273 K and 0.1 MPa, Fig. S29†) also favor the capture and enrichment of CO₂ within porous solid catalysts during the reaction.

Based on previous reports, our experimental results and above analyses, a plausible synergistic catalytic mechanism was afforded for CO₂ conversion with epoxides over the catalyst Phen⁺-PHP-2Br, as shown in Scheme 3. First, the epoxide substrate was together activated by multiple active sites including POSS-derived Si–OH groups, a small amount of absorbed water and some active radical N atoms from Phen moieties, greatly leading to the ring opening of the epoxide *via* hydrogen-bond interaction and C–O bond polarization.^{23,25,56,57} Then, the nucleophilic Br[−] anion attacked the less hindered β-carbon of the activated epoxide to create an oxanion intermediate stabilized by multiple –OH HBD groups.^{23,53} Subsequently, the oxanion intermediate interacted with the inserted CO₂ molecules to form the bromoalkyl-carbonate anion intermediate.^{22,23,53} Finally, the product cyclic carbonate was formed by intramolecular ring-closure of the carbonate anion intermediate with the release of Br[−] anions, following with the regeneration of the catalyst.

Conclusions

In summary, a new series of phenanthroline cationic radical porous hybrid polymers were constructed by the Heck reaction between newly-designed phenanthroline ionic monomers and VPOSS units. The obtained Phen⁺-PHPs have desired porous structures with moderate surface areas and possess multiple catalytically active sites, which could be regarded as metal-free heterogeneous catalysts for both oxidation of sulfides and chemical fixation of CO₂. Owing to its unique cationic radical redox character, the typical catalyst Phen⁺-PHP-2 exhibited remarkable heterogeneous catalytic activities in the selective oxidation of sulfides to sulfoxides using a green oxidant H₂O₂

under mild conditions. Besides, the extended catalyst Phen⁺-PHP-2Br could be also used as a highly efficient metal-free heterogeneous catalyst for the conversion of CO₂ with epoxides into cyclic carbonates under atmospheric pressure, which is attributed to the synergistic catalysis effect of nucleophilic Br⁻ anions and N active atoms within Phen radical moieties and HBD active sites including Si-OH groups and H-bonded water. This work affords a general route to construct more new multifunctional cationic radical porous polymers for diverse applications in metal-free heterogeneous catalysis and related energy storage and conversion.

Conflicts of interest

There are no conflicts to declare.

Acknowledgements

This work was supported by the National Natural Science Foundation of China (21603089, 21706106 and 21503098), the Natural Science Foundation of Jiangsu Province (BK20160209), the Natural Science Foundation of Jiangsu Higher Education Institutions of China (16KJB150014), the Postgraduate Research & Practice Innovation Program of Jiangsu Province (KYCX20_2357 and KYCX20_2354) and the Top-notch Academic Programs Project of Jiangsu Higher Education Institutions (TAPP).

Notes and references

- Z. Ji, T. Li and O. M. Yaghi, *Science*, 2020, **369**, 674–780.
- J. Wu, F. Xu, S. Li, P. Ma, X. Zhang, Q. Liu, R. Fu and D. Wu, *Adv. Mater.*, 2019, **31**, 1802922.
- I. Ratera and J. Veciana, *Chem. Soc. Rev.*, 2012, **41**, 303–349.
- N. Zhang, S. R. Samanta, B. M. Rosen and V. Percec, *Chem. Rev.*, 2014, **114**, 5848–5958.
- K. Kato and A. Osuka, *Angew. Chem., Int. Ed.*, 2019, **58**, 8978–8986.
- J.-K. Sun, Y.-J. Zhang, G.-P. Yu, J. Zhang, M. Antonietti and J. Yuan, *J. Mater. Chem. C*, 2018, **6**, 9065–9070.
- X. Yu, J. Sun, J. Yuan, W. Zhang, C. Pan, Y. Liu and G. Yu, *Chem. Eng. J.*, 2018, **350**, 867–871.
- Y. Jiang, I. Oh, S. H. Joo, O. Buyukcakir, X. Chen, S. H. Lee, M. Huang, W. K. Seong, J. H. Kim, J. Rohde, S. K. Kwak, J.-W. Yoo and R. S. Ruoff, *ACS Nano*, 2019, **13**, 5251–5258.
- H. Phan, T. S. Heng, D. Wang, X. Li, W. Zeng, J. Ding, K. P. Loh, A. T. S. Wee and J. Wu, *Chem*, 2019, **5**, 1223–1234.
- F. Xu, H. Xu, X. Chen, D. Wu, Y. Wu, H. Liu, C. Gu, R. Fu and D. Jiang, *Angew. Chem., Int. Ed.*, 2015, **54**, 6814–6818.
- S. Wu, M. Li, H. Phan, D. Wang, T. S. Heng, J. Ding, Z. Lu and J. Wu, *Angew. Chem., Int. Ed.*, 2018, **57**, 8007–8011.
- Z. Mi, P. Yang, R. Wang, J. Unruangsri, W. Yang, C. Wang and J. Guo, *J. Am. Chem. Soc.*, 2019, **141**, 14433–14442.
- H. A. Beejapur, Q. Zhang, K. Hu, L. Zhu, J. Wang and Z. Ye, *ACS Catal.*, 2019, **9**, 2777–2830.
- T. Škorjanc, D. Shetty, M. A. Olson and A. Trabolsi, *ACS Appl. Mater. Interfaces*, 2019, **11**, 6705–6716.
- G. Chen, Y. Zhou, X. Wang, J. Li, S. Xue, Y. Liu, Q. Wang and J. Wang, *Sci. Rep.*, 2015, **5**, 11236.
- P. Zhang, Z.-A. Qiao, X. Jiang, G. M. Veith and S. Dai, *Nano Lett.*, 2015, **15**, 823–828.
- G. Chen, W. Hou, J. Li, X. Wang, Y. Zhou and J. Wang, *Dalton Trans.*, 2016, **45**, 4504–4508.
- C. Hua, B. Chan, A. Rawal, F. Tuna, D. Collison, J. M. Hook and D. M. D'Alessandro, *J. Mater. Chem. C*, 2016, **4**, 2535–2544.
- O. Buyukcakir, S. H. Je, D. S. Choi, S. N. Talapaneni, Y. Seo, Y. Jung, K. Polychronopoulou and A. Coskun, *Chem. Commun.*, 2016, **52**, 934–937.
- O. Buyukcakir, S. H. Je, S. N. Talapaneni, D. Kim and A. Coskun, *ACS Appl. Mater. Interfaces*, 2017, **9**, 7209–7216.
- G. Das, T. Skorjanc, S. K. Sharma, F. Gandara, M. Lusi, D. S. S. Rao, S. Vimala, S. K. Prasad, J. Raya, D. S. Han, R. Jagannathan, J.-C. Olsen and A. Trabolsi, *J. Am. Chem. Soc.*, 2017, **139**, 9558–9565.
- G. Chen, X. Huang, Y. Zhang, M. Sun, J. Shen, R. Huang, M. Tong, Z. Long and X. Wang, *Chem. Commun.*, 2018, **54**, 12174–12177.
- Y. Zhang, K. Liu, L. Wu, H. Zhong, N. Luo, Y. Zhu, M. Tong, Z. Long and G. Chen, *ACS Sustainable Chem. Eng.*, 2019, **7**, 16907–16916.
- S. Hou, N. Chen, P. Zhang and S. Dai, *Green Chem.*, 2019, **21**, 1455–1460.
- G. Chen, Y. Zhang, J. Xu, X. Liu, K. Liu, M. Tong and Z. Long, *Chem. Eng. J.*, 2020, **381**, 122765.
- C.-A. Wang, K. Nie, G.-D. Song, Y.-W. Lia and Y.-F. Han, *RSC Adv.*, 2019, **9**, 8239–8245.
- G. H. Gunasekar and S. Yoon, *J. Mater. Chem. A*, 2019, **7**, 14019–14026.
- K. Kim, O. Buyukcakir and A. Coskun, *RSC Adv.*, 2016, **6**, 77406–77409.
- J. Byun, H. A. Patel, D. Thirion and C. T. Yavuz, *Polymer*, 2017, **126**, 308–313.
- Y. Zhang, K. Zhang, L. Wu, K. Liu, R. Huang, Z. Long, M. Tong and G. Chen, *RSC Adv.*, 2020, **10**, 3606–3614.
- S. Wang, L. Tan, C. Zhang, I. Hussain and B. Tan, *J. Mater. Chem. A*, 2015, **3**, 6542–6548.
- M. Ge and H. Liu, *J. Mater. Chem. A*, 2016, **4**, 16714–16722.
- Y. Zhang, N. Luo, J. Xu, K. Liu, S. Zhang, Q. Xu, R. Huang, Z. Long, M. Tong and G. Chen, *Dalton Trans.*, 2020, **49**, 11300–11309.
- D. Wang, S. Feng and H. Liu, *Chem. - Eur. J.*, 2016, **22**, 14319–14327.
- B. Li, Z. Guan, X. Yang, W. D. Wang, W. Wang, I. Hussain, K. Song, B. Tan and T. Li, *J. Mater. Chem. A*, 2014, **2**, 11930–11939.
- G. Das, T. Prakasam, S. Nuryyeva, D. S. Han, A. Abdel-Wahab, J.-C. Olsen, K. Polychronopoulou, C. P. Iglesias, F. Ravoux, M. Jouiadf and A. Trabolsi, *J. Mater. Chem. A*, 2016, **4**, 15361–15369.
- P. Cao, Y. Li, Y. Li, X. Zhang, X. Wang and Z. Jiang, *Sustainable Energy Fuels*, 2020, **4**, 2236–2248.

- 38 F. Tzompantzia, C. Tzompantzi-Flores, N. S. Portillo-Vélez, J. C. Castillo-Rodríguez, R. Gómez, R. P. Hernández and C. E. Santolalla-Vargas, *Fuel*, 2020, **281**, 118471.
- 39 R. K. Arvela, N. E. Leadbeater, M. S. Sangi, V. A. Williams, P. Granados and R. D. Singer, *J. Org. Chem.*, 2005, **70**, 161–168.
- 40 S. Kim, B. Kim, N. A. Dogan and C. T. Yavuz, *ACS Sustainable Chem. Eng.*, 2019, **7**, 10865–10872.
- 41 H. Liu, R. Sun, S. Feng, D. Wang and H. Liu, *Chem. Eng. J.*, 2019, **359**, 436–445.
- 42 I. Fernández and N. Khiar, *Chem. Rev.*, 2003, **103**, 3651–3705.
- 43 P. Zhao, M. Zhang, Y. Wu and J. Wang, *Ind. Eng. Chem. Res.*, 2012, **51**, 6641–6647.
- 44 Q. Zhou, M. Ye, W. Ma, D. Li, B. Ding, M. Chen, Y. Yao, X. Gong and Z. Hou, *Chem. - Eur. J.*, 2019, **25**, 4206–4217.
- 45 P. Ménová, F. Kafka, H. Dvorská, S. Gunnoo, M. Šanda and R. Cibulka, *Adv. Synth. Catal.*, 2011, **353**, 865–870.
- 46 T. Hartman, J. Šturala and R. Cibulka, *Adv. Synth. Catal.*, 2015, **357**, 3573–3586.
- 47 J. Šturala, S. Boháčová, J. Chudoba, R. Metelková and R. Cibulka, *J. Org. Chem.*, 2015, **80**, 2676–2699.
- 48 W. Hao, D. Chen, Y. Li, Z. Yang, G. Xing, J. Li and L. Chen, *Chem. Mater.*, 2019, **31**, 8100–8105.
- 49 J. Li, Y. Chen, X. Yang, S. Gao and R. Cao, *J. Catal.*, 2020, **381**, 579–589.
- 50 M. Liu, X. Wang, Y. Jiang, J. Sun and M. Arai, *Catal. Rev.: Sci. Eng.*, 2019, **61**, 214–269.
- 51 R. R. Shaikh, S. Pornpraprom and V. D'Elia, *ACS Catal.*, 2018, **8**, 419–450.
- 52 S. Subramanian, Y. Song, D. Kim and C. T. Yavuz, *ACS Energy Lett.*, 2020, **5**, 1689–1700.
- 53 A. M. Hardman-Baldwin and A. E. Mattson, *ChemSusChem*, 2014, **7**, 3275–3278.
- 54 J. Wang, J. Leong and Y. Zhang, *Green Chem.*, 2014, **16**, 4515–4519.
- 55 M. Liu, L. Liang, X. Li, X. Gao and J. Sun, *Green Chem.*, 2016, **18**, 2851–2863.
- 56 Y. Zhang, G. Chen, L. Wu, K. Liu, H. Zhong, Z. Long, M. Tong, Z. Yang and S. Dai, *Chem. Commun.*, 2020, **56**, 3309–3312.
- 57 K. R. Roshan, R. A. Palissery, A. C. Kathalikkattil, R. Babu, G. Mathai, H.-S. Leed and D.-W. Park, *Catal. Sci. Technol.*, 2016, **6**, 3997–4004.
- 58 M. Alves, B. Grignard, R. Mereau, C. Jerome, T. Tassaing and C. Detrembleur, *Catal. Sci. Technol.*, 2017, **7**, 2651–2684.
- 59 S. Subramanian, J. Park, J. Byun, Y. Jung and C. T. Yavuz, *ACS Appl. Mater. Interfaces*, 2018, **10**, 9478–9484.
- 60 Y. Zhou, W. Zhang, L. Ma, Y. Zhou and J. Wang, *ACS Sustainable Chem. Eng.*, 2019, **7**, 9387–9398.
- 61 Y.-M. Li, L. Yang, L. Sun, L. Ma, W.-Q. Deng and Z. Li, *J. Mater. Chem. A*, 2019, **7**, 26071–26076.
- 62 X. Wang, Q. Dong, Z. Xu, Y. Wu, D. Gao, Y. Xu, C. Ye, Y. Wen, A. Liu, Z. Long and G. Chen, *Chem. Eng. J.*, 2021, **403**, 126460.
- 63 X. Wang, Y. Zhou, Z. Guo, G. Chen, J. Li, Y. Shi, Y. Liu and J. Wang, *Chem. Sci.*, 2015, **6**, 6916–6924.
- 64 J. Li, D. Jia, Z. Guo, Y. Liu, Y. Lyu, Y. Zhou and J. Wang, *Green Chem.*, 2017, **19**, 2675–2686.
- 65 S. Subramanian, J. Oppenheim, D. Kim, T. S. Nguyen, W. M. H. Silo, B. Kim, W. A. Goddard III and C. T. Yavuz, *Chem*, 2019, **5**, 3232–3242.
- 66 R. Luo, X. Liu, M. Chen, B. Liu and Y. Fang, *ChemSusChem*, 2020, **13**, 3945–3966.
- 67 Z. Guo, Q. Jiang, Y. Shi, J. Li, X. Yang, W. Hou, Y. Zhou and J. Wang, *ACS Catal.*, 2017, **7**, 6770–6780.
- 68 Y. Chen, R. Luo, J. Bao, Q. Xu, J. Jiang, X. Zhou and H. Ji, *J. Mater. Chem. A*, 2018, **6**, 9172–9182.
- 69 D. Ma, K. Liu, J. Li and Z. Shi, *ACS Sustainable Chem. Eng.*, 2018, **6**, 15050–15055.
- 70 K. Hu, Y. Tang, J. Cui, Q. Gong, C. Hu, S. Wang, K. Dong, X. Meng, Q. Sun and F.-S. Xiao, *Chem. Commun.*, 2019, **55**, 9180–9183.